Structural investigation of the stability in temperature of some high entropy alloys as a function of their electronic structure

M. Calvo-Dahlborg, U. Dahlborg, J. Cornide, S. Mehraban, Z. Leong, T.C. C Hansen, R.K. K Wunderlich, R. Goodall, N.P. P Lavery, S.G.R. G R Brown

Structural investigation of the stability in temperature of some high entropy alloys as a function of their electronic structure

M. Calvo-Dahlborg[1,2,*], U. Dahlborg[1,2], J. Cornide[1], S. Mehraban[2], Z. Leong[3], T.C. Hansen[4], R.K. Wunderlich[5], R. Goodall[3], N.P. Lavery[2], S.G.R. Brown[2]

[1] GPM, CNRS-UMR6634, University of Rouen Normandie, Campus Madrillet, BP12, 76801 St-Etienne-du-Rouvray, France.
monique.calvo-dahlborg@univ-rouen.fr, ulf.dahlborg@univ-rouen.fr.

[2] College of Engineering, Swansea University, Bay Campus, Fabian Way, Skewen, Swansea SA1 8EN, UK.
s.mehraban@swansea.ac.uk, n.p.lavery@swansea.ac.uk, s.g.r.brown@swansea.ac.uk.

[3] Department of Materials Science and Engineering, Sir Robert Hadfield Building, Mappin Street, Sheffield, S1 3JD, UK. zhaoyuan@sheffield.ac.uk, r.goodall@sheffield.ac.uk

[4] Institut Laue Lagnevin, 71 Avenue des Martyrs 38042 Grenoble Cedex 9, France.
hansen@ill.fr

[5] Institut für funktionelle Nanosysteme, Universität Ulm, Albert-Einstein-Allee 47 D-89081 Ulm, Germany. rainer.wunderlich@uni-ulm.de.

* Corresponding author: monique.calvo-dahlborg@univ-rouen.fr.

Abstract:

High Entropy Alloys (HEA) can be classified in three domains according to their e/a and r values, with e/a, the number of itinerant valence electrons and r the average radius for a 12 nearest atoms neighborhood. The phase composition, thermal stability and possible phase transformations of a series of HEA alloys, $CoCr_zFeNi$-XY (with X and Y = Al, Cu, Pd, Ru, Ti and z=0 or 1), selected according to their e/a ratio were investigated in cast conditions (T0), after 3 hours homogenization at 1100°C (T1) and after 3 hours annealing at 700°C (T3). It is observed that for the alloys from domain I which contains fcc structures, the microstructure transforms from multi- to almost single-phase under homogenization (T1). In domain III alloys contains cubic (bcc and/or B2) structures very small multi-structural changes are observed. Alloys in domain II have mixed structure, i.e. several different structures in the diffraction pattern, which changes during heat treatments.

Keywords: High Entropy Alloys, multicomponent, structure, phases, calorimetry, e/a

1. Introduction

The term “high entropy alloys” (HEA) was introduced in 2004 to designate alloys consisting of 5 or more principal elements in equi- or near-equimolar amounts (5 to 35at%), being single-phased and having simple crystalline structures [1]. The notion of high entropy refers to their high entropy of mixing. The last 15 years the alloys have been intensely investigated with respect to phase composition, microstructure, as well as thermal, magnetic and mechanical properties. However, it has also been shown that due to the unique combination of crystalline structures and microstructures several HEA can outnumber alloys today used in specific technological applications [2-5]. Thus, a new kind of metallurgy has emerged in that all elements have to be considered on an equal footing during the solidification process. This is different as compared to traditional technical alloys which usually consist of a leading ternary or binary system, such as for example Ti-Al, while the other elements are to be considered as minor additions. Thus, the designation, “multi-principal element alloys”, is also used to define these kind of alloys [1,6].

It is now well established that HEAs can be single-structured but not, or almost never, single-phased [10]. The identified structures belong in most cases to the cubic close-packed (fcc-type), the body centered cubic (bcc-type) and also hexagonal close packed (hcp-type) families of structures. It should though be noted that the identification of crystalline structures present in a many-phase alloy is a very complicated matter and its success depends on the resolution of the utilized experimental technique. Since their discovery the determination of the phase stability of HEAs after solidification has been a significant issue in many investigations. Phase changes due to external fields (temperature, pressure, etc) have been found to have a profound influence on the microstructure and, thus, the mechanical and magnetic properties. The design of alloys that contain phases with specific crystalline structures is accordingly of utmost importance in order to predict physical properties. For this purpose, a combination of parameters relevant in this connection have been considered including aspects of

definition/terminology, phase formation, microstructure and phase stability, strengthening mechanisms, and high temperature properties, as well as the density and cost [2-5, 7-9].

Recently a classification of HEAs was proposed using the average value of the electron concentration or number of itinerant electrons per atom (e/a) in the alloy and the average atomic radius calculated for a 12-atoms atomic neighbourhood [11, 12]. The importance of the number of itinerant electrons per atom to understand and predict the phases in solid solutions has been stressed as early as 1966 [13]. In [14] the use of e/a is discussed by Massalski for the determination of crystalline Hume-Rothery phases as opposed to an approach using the total number of valence electrons (VEC) (which includes the d electrons). By applying this approach for HEAs as solid solutions a classification and design methodology was proposed. From the variation of the average magnetic moment per atom and the hardness as a function of e/a and the 12 atoms radius, three domains could be identified in [11] and [12]: one domain containing alloys with phases with close-packed cubic structures (below denoted fcc), a second one was found to contain alloys with phases of a mixed and complex structural type and a third one containing alloys with phases with body-centered cubic structures (below denoted bcc). The atomic radii are taken from Teatum [15] as these probably are the most useful when discussing metallic alloys. They are reported for a coordination number 12 atomic surrounding and were obtained from observed atomic distances in face-centered cubic and hexagonal close-packed structures. The first property used for classification of HEA's was the magnetization at saturation [11, 12].

The success of using high entropy alloys in most technological applications depends on their stability following different thermal exposures. The present work focusses on the influence of heat treatments on the stability of alloys and aims to investigate common effects in the three different domains after heat treatments. The alloys chosen for this investigation cover all domains according to the classification in [11, 12] and all contain Co, Fe and Ni as base

components (abbreviated to CFN below). When Cr is also present in an alloy the abbreviation CCFN is used.

2. Material and methods

All alloys were prepared by arc melting of pure elements, with purities higher than 99.9 wt.%, under a Ti-gettered high-purity argon atmosphere [10]. The alloys were remelted several times in order to obtain homogeneity and to minimize oxide impurities. Cylindrical rods with diameter of 3mm were then prepared by copper-mold suction casting into a water-cooled Cu hearth.

Table 1 gives the acronyms and the nominal compositions of the investigated alloys.

Acronym	Alloy nominal composition (at.%)
CCFNPd	$Co_{20}Cr_{20}Fe_{20}Ni_{20}Pd_{20}$
CCFNRu	$Co_{20}Cr_{20}Fe_{20}Ni_{20}Ru_{20}$
CCFNCu	$Co_{20}Cr_{20}Fe_{20}Ni_{20}Cu_{20}$
CFNCu	$Co_{25}Fe_{25}Ni_{25}Pd_{25}$
CCFNAl	$Co_{20}Cr_{20}Fe_{20}Ni_{20}Al_{20}$
CCFNAlCu	$Co_{16.6}Cr_{16.6}Fe_{16.6}Ni_{16.6}Al_{16.6}Cu_{16.6}$
CFNTi	$Co_{25}Fe_{25}Ni_{25}Ti_{25}$
CCFNAlTi	$Co_{16.6}Cr_{16.6}Fe_{16.6}Ni_{16.6}Al_{16.6}Ti_{16.6}$
CFNAl	$Co_{25}Fe_{25}Ni_{25}Al_{25}$
CFNAlTi	$Co_{20}Cr_{20}Fe_{20}Ni_{20}Ti_{20}$
$CCFNAl_{1.2}$	$Co_{19.2}Cr_{19.2}Fe_{19.2}Ni_{19.2}Al_{23.1}$
$CF_{0.8}NAl_{1.2}$	$Co_{25}Fe_{20}Ni_{25}Al_{30}$

In order to investigate their thermal stability, the as-cast alloys were subjected to different heat treatments. Samples cut from the same ingots were annealed for 3 hours at 1100°C

(T1), 700°C (T3) or 400°C (T2). In the following the temperature at which the samples had been heat treated will be referred to as T1, T2 and T3, the as-cast conditions as T0. The time needed to reach the required temperature was some few minutes. The heat-treated alloys were ice-water quenched in order to retain the structure. All subsequent measurements were performed at ambient temperature.

The crystalline structure of all samples was investigated by neutron diffraction (ND) on the D20 diffractometer at Institut Laue-Langevin (ILL), Grenoble (France). The wavelength of the incident neutrons was 1.12Å. The crystalline structure of the phases present in the alloys were determined by a refinement procedure using the DICVOL computer code [16]. The values of the lattice constants will be presented in a separate paper. As neutrons are weakly interacting with matter the refinement gives a result valid for the entire irradiated volume.

The phase transformations occurring during heating up to different temperatures and during the subsequent cooling were studied for some selected alloys by Differential Scanning Calorimetry (DSC) with a Netzsch STA 449 C instrument under a flowing nitrogen protective atmosphere. The rate of temperature change was in all measurements $40 K min^{-1}$. It will be called "slow" in the following as opposition to "quench" for the water quench.

3. Results

3.1 Determination of the crystallographic structure of as-cast and annealed alloys by neutron diffraction

The structure of 12 selected alloys, 4 in each of the three domains that were defined in [12], will be discussed in this work. All have been investigated in as-cast condition as well as after two different heat treatments, namely T1 and T3. The measured diffraction patterns are presented in Fig. 1 to 3. For clarity the three curves for the different heat treatments have been shifted vertically and presented in the following order, from bottom to top: as-cast alloys (T0), after annealing for 3h at 1100°C (T1) and after annealing for 3h at 700°C (T3). When comparing

the diffraction patterns, it is important to note that in the experiments the samples, all being ingots of different shapes and sizes, have been held in arbitrary orientations. Thus, the measured diffraction peak intensities are also affected by texture and they will therefore not necessarily give a representative estimation of the amount of a certain phase present. It should also be noted that all alloys have been produced and treated in the same way. Thus, no significant influence on the alloy phase composition due to a variation of elemental purities or on differences in cooling rates on diffraction peak intensities is expected.

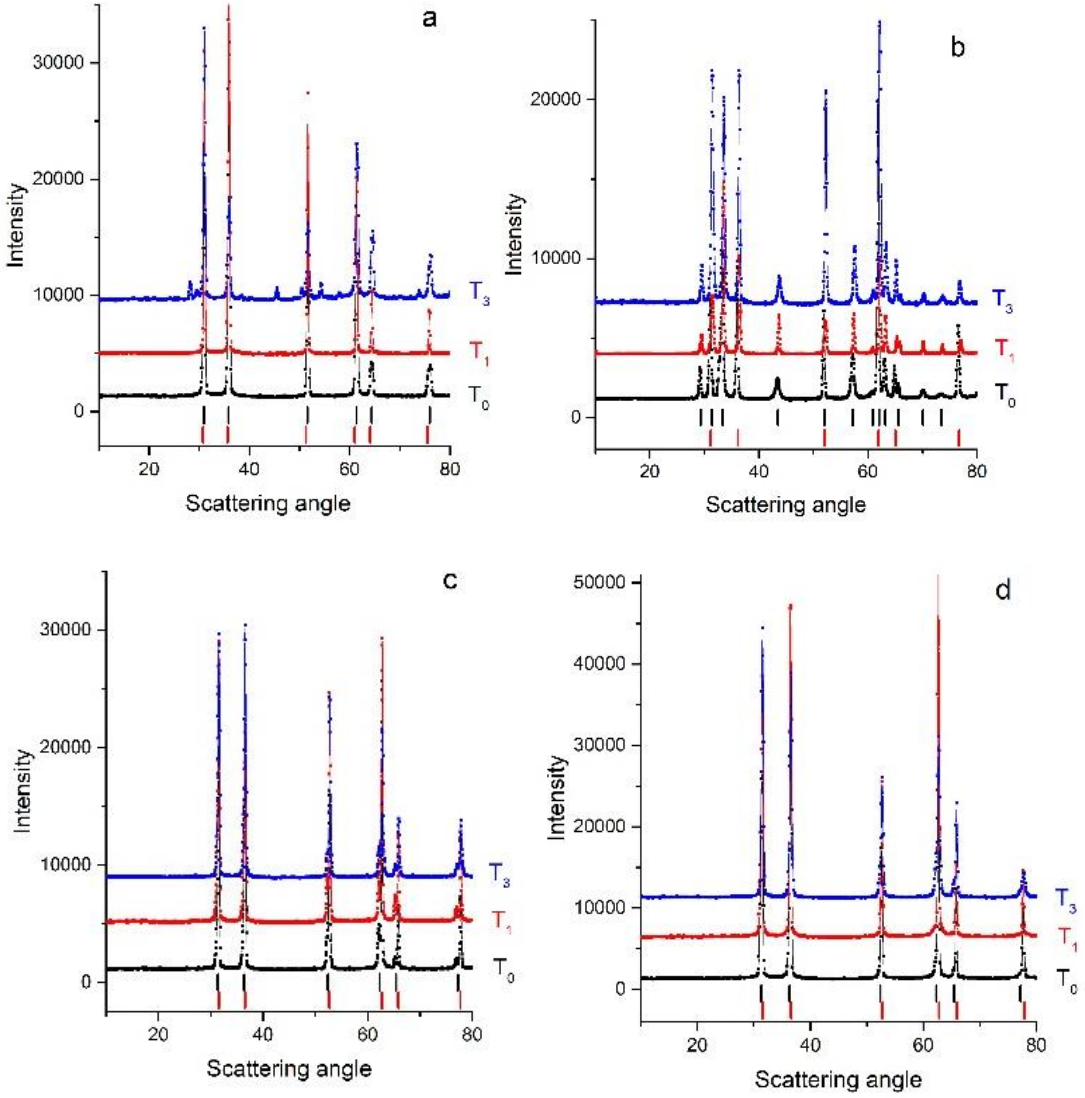

Fig. 1: ND patterns of the investigated alloys of Domain I in (black) the as-cast (T0) and after heat treatment at (red) T1 and (blue) T3 condition. The alloy compositions are a) CoCrFeNiPd, b) CoCrFeNiRu, c) CoCrFeNiCu, and d) CoFeNiCu. The vertical bars correspond to diffraction peak positions of the two crystalline structures present in largest amounts in every alloy.

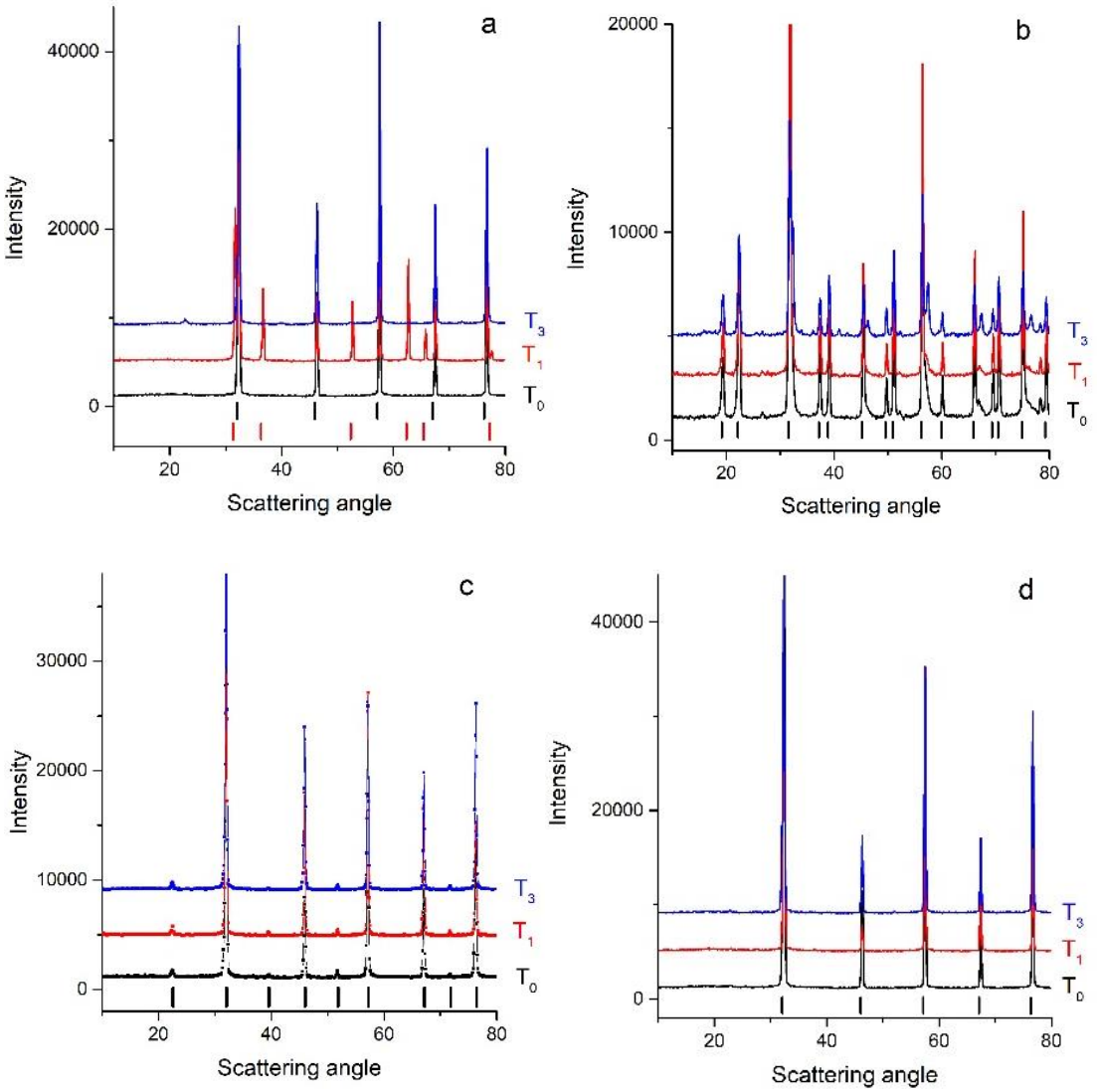

Fig. 2: ND patterns of the investigated alloys of Domain III in (black) the as-cast (T0) and after heat treatment at (red) T1 and (blue) T3 condition.The alloy compositions are a) CoFeNiAl, b) CoFeNiAlTi, c) $CoCrFeNiAl_{1.2}$, and d) $CoFe_{0.8}NiAl_{1.2}$. The vertical bars correspond to diffraction peak positions of the two crystalline structures present in largest amounts in every alloy.

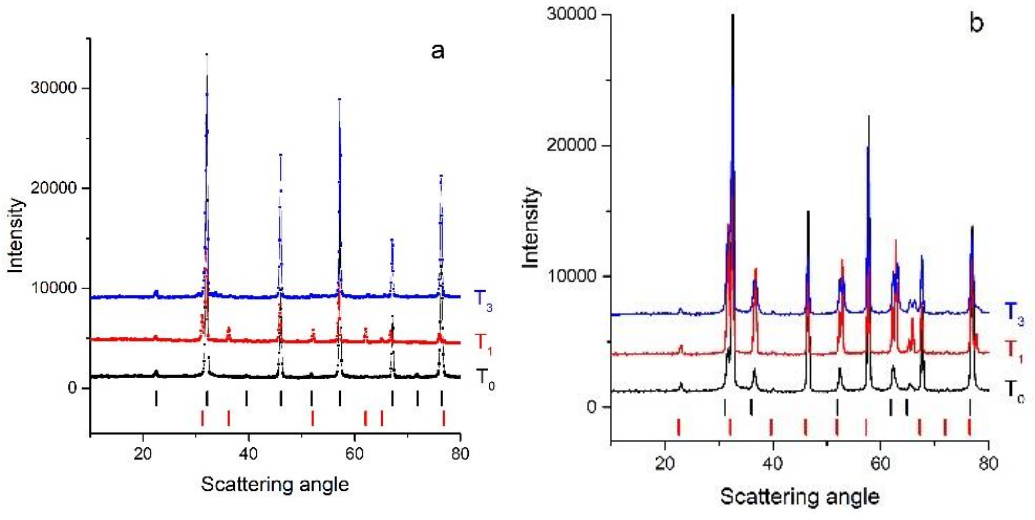

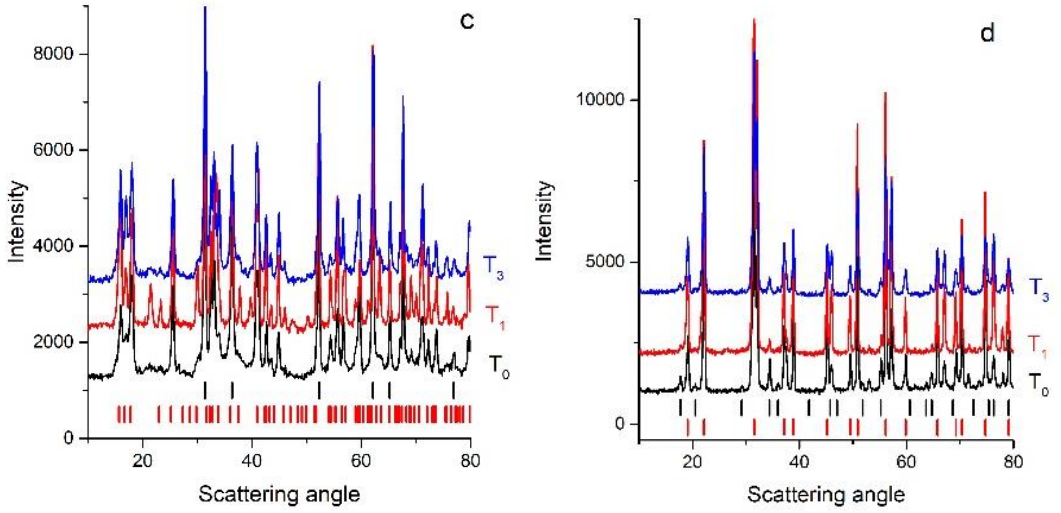

Fig. 3: ND patterns of the investigated alloys of Domain II in (black) the as-cast (T0) and after heat treatment at (red) T1 and (blue) T3 condition. The alloy compositions are a) CoCrFeNiAl, b) CoCrFeNiAlCu, c) CoFeNiTi and d) CoCrFeNiAlTi. The vertical bars correspond to diffraction peak positions of the two crystalline structures present in largest amounts in every alloy.

The structures identified from the diffraction patterns displayed in Figs 1 to 3 are listed in Table 2. A relative rough estimate of the amount of a particular structure in columns T0, T1 and T3 is given from their positions left to right, the one to the left being the main one. As the elemental composition of the different phases/structures has not been determined with enough accuracy only the type of crystalline structure is given. The question marks indicate the presence of a trace structure that could not be identified. The first column in Table 2 indicates the domain to which the alloy belongs according to the classification mentioned above [11, 12]. It can be seen that several alloys exhibit two phases having the same type of structure, for examples two simple fcc and one bcc in combination with a B2. The derived lattice constants of the different structures are presented in other works [10, 17, 18].

Table 2: List of the crystalline structures observed in alloys in as-cast condition (T0) as well as after heat treatments T1 and T3 defined in the text. The specified structures are the simple face-centered cubic (fcc), the simple body-centered cubic (bcc), the ordered body-centered cubic (B2), the Heusler ($L2_1$), and the hexagonal close-packed (hcp) structural type. The presence of unidentified structure is denoted by (?). The first column indicates the domain to which the alloy belongs according to the classification discussed in [11, 12].

Domain	Alloy	As-cast (T0)				After annealing (T1)				After annealing (T3)			
I	CCFNPd	fcc	fcc			fcc				fcc	fcc	?	
	CCFNRu	hcp	fcc			hcp	fcc			hcp	fcc		
	CCFNCu	fcc	fcc			fcc	fcc			fcc	fcc		
	CFNCu	fcc	fcc			fcc	fcc			fcc	fcc		
II	CCFNAl	bcc	fcc	B2		bcc	fcc	B2		bcc	B2	?	
	CCFNAlCu	bcc	fcc	B2		bcc	fcc	fcc	B2	bcc	fcc	fcc	B2
	CFNTi	hcp	fcc	?		hcp	fcc	?		hcp	fcc	?	
	CCFNAlTi	$L2_1$	$L2_1$	fcc	bcc	$L2_1$	bcc	?		$L2_1$	$L2_1$	fcc	bcc
III	CFNAl	bcc	B2			bcc	fcc			bcc	B2		
	CFNAlTi	$L2_1$	?			$L2_1$	?			$L2_1$	?		
	$CCFNAl_{1.2}$	bcc	B2			bcc	B2			bcc	B2		
	$CF_{0.8}NAl_{1.2}$	bcc				bcc				bcc	B2		

All the alloys belonging to a specific domain have been found to have the type of structure in the as-cast state as predicted by the classification in [12]. Thus, in domain I alloys with fcc or hcp structures are found while the alloys in domain III contain structures of bcc type. The alloys in domain II form structures with both fcc and bcc type. The $L2_1$ phase is observed for a few alloy compositions and also after different heat treatments. It is a complex structure and contains atoms in both octahedral and tetrahedral interstitial positions with all atoms located on the sites of a body-centered cubic lattice.

On heat treatment it can be seen that the alloys of a particular domain behave similarly. The investigated alloys of Domain I retain fcc and hcp phases after both T1 and T3 heat treatments (see Fig.1 a to d). Alloys of Domain III retain phases of bcc types (see Fig 2 a to d) and alloys of Domain II retain their mixed phase composition (see Fig. 3 a to d). Another result from Table 2 is that removing Cr from one alloy sometimes drives the alloy from one Domain

to another (e.g. CCFNAlTi and CCFNAl in domain II, CFNAlTi and CFNAl in Domain III) and sometimes not (e.g. CCFNCu and CFNCu in Domain I). It is also interesting to note that a small change in the relative Al amount of an alloy can have the same effect (e.g. CCFNAl in Domain II and $CCFNAl_{1.2}$ in Domain III). Both these effects depend on compared values of e/a and r [12].

3.2 Calorimetric studies

In order to obtain further information on the thermal stability of the alloy structures differential scanning calorimetry (DSC) measurements were performed on one alloy from each Domain: CCFNPd from Domain I, CCFNAl from Domain II and CFNAl from Domain III. The heating/cooling rate was $40Kmin^{-1}$ for all measurements and all measurements were performed under continuous nitrogen gas flow. It should be noted that all studied alloys have melting points above 1400°C and that the solidification takes place during a slow cooling. The alloys were investigated according to different heat treatment schemes:

- A. Heating from room temperature (RT) to 1500°C on an as-cast sample previously annealed 3h at 1100°C and subsequently water-quenched.
- B. Heating from RT to 1500°C on an as-cast sample previously annealed 3h at 700°C and subsequently water-quenched.
- C_i (i=1,3). Heating/cooling of an as-cast sample according to the temperature variational scheme shown in Fig 4. That is:
    - C_1: Heating of an as-cast sample from RT to 1100°C and subsequently cooled at the same rate (40K/min).
    - C_2: Heating of sample C_1 from RT to 700°C and subsequently cooled at the same rate (40K/min).
    - C_3: Heating of sample C_2 from RT to 1500°C.

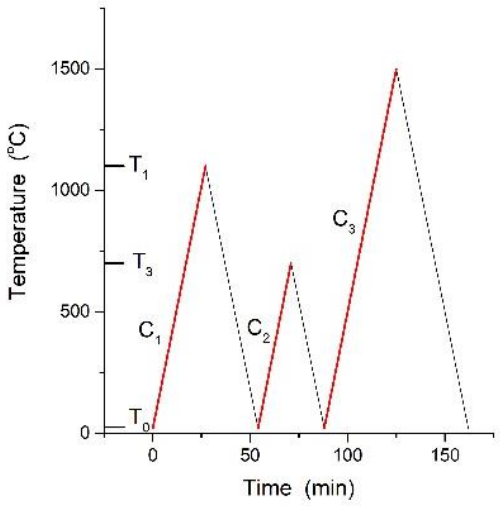

Fig. 4. Temperature variational scheme applied during DSC measurements of as-cast alloys previously heated to 1100°C and subsequently cooled with a rate of 40K/min.

The heat flow curves for Domains I, III and II, measured during heating, are shown in Fig. 5a, 6a and 7a while the differentiated counterparts are displayed in Fig. 5b, 6b and 7b, respectively. The differentiated curves help in detecting occurrences of specific features and also highlight a comparison. Several phase transformations obviously occur in all alloys during the different heating schemes. Main structural events are defined to take place by a temperature change in the observed curves of more than ~0.2°C during 10 seconds. The heating rate in all measurements was 40K/min. Some small anomalies are nevertheless considered to be real if they are observed in several DSC heat flow curves.

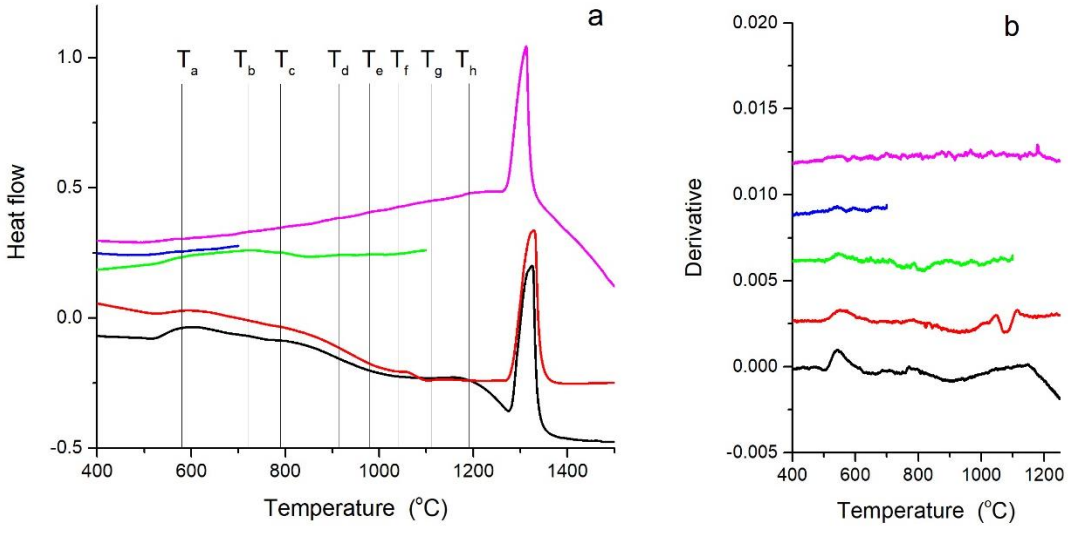

Fig. 5: (a) DSC heat flow curves and (b) their derivative measured during the five different temperature schemes for the CCFNPd alloy belonging to domain I. The curves are shifted vertically in the following order from bottom: Scheme A (black), scheme B (red), scheme C_1 (green), scheme C_2 (blue), scheme C_3 (magenta). The vertical lines correspond approximately to the average temperature in the corresponding column in table 3.

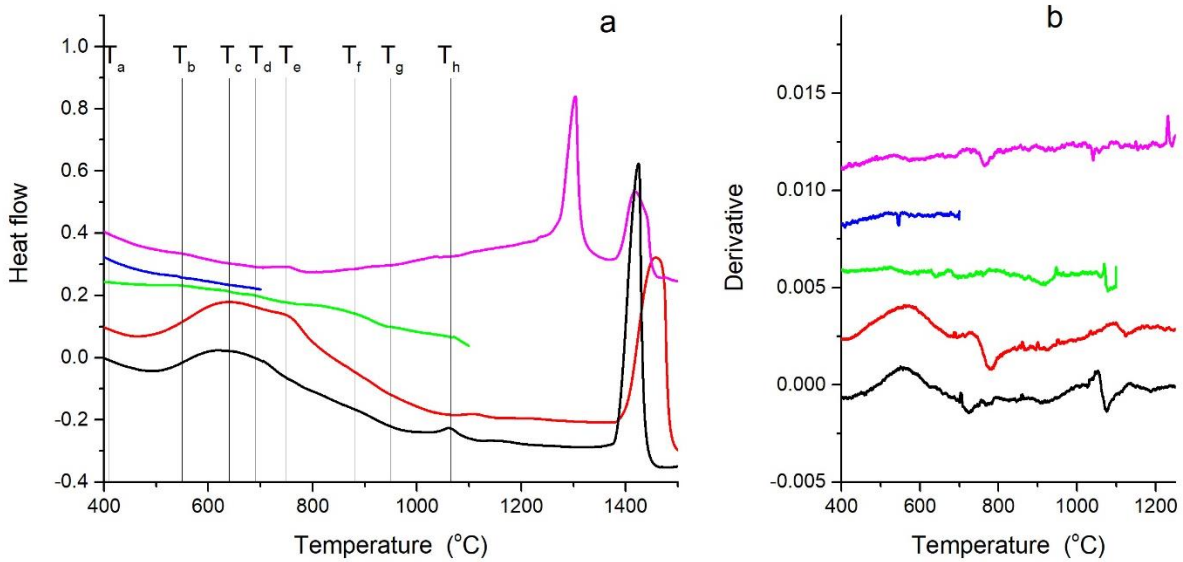

Fig. 6: (a) DSC heat flow curves and (b) their derivative obtained for the five different temperature schemes for the CFNAl alloy belonging to domain III. The curves are shifted vertically in the following order from bottom: A (black), B (red), C (green), D (blue), E (magenta). The vertical lines correspond approximately to the average temperature in the corresponding column in table 4.

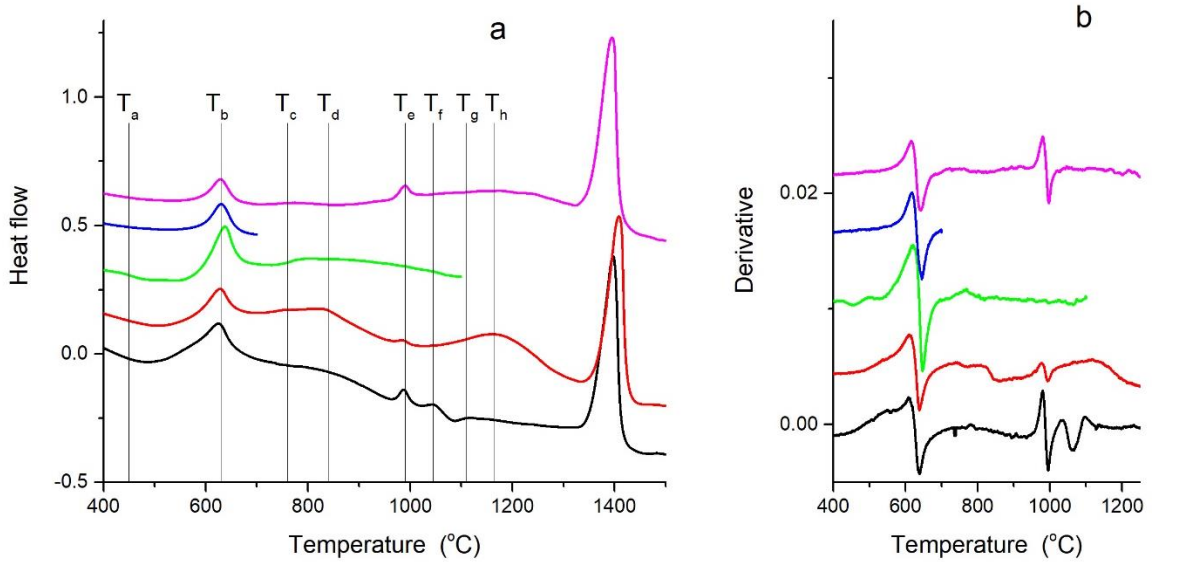

Fig. 7: (a) DSC heat flow curves and (b) their derivative obtained for the five different temperature schemes for the CCFNAl alloy belonging to domain II. The curves are shifted vertically in the following order from bottom: A (black), B (red), C (green), D (blue), E (magenta). The vertical lines correspond approximately to the average temperature in the corresponding column in table 5.

4. Discussion

When comparing and interpreting the diffraction measurements in combination with the DSC studies it should be realized that the alloys have not been investigated under completely comparable circumstances by the two techniques. For experimental reasons the maximum temperature achievable in the neutron diffraction measurements was too low in order to duplicate the DSC measurements. Thus, all diffraction measurements were conveniently performed at ambient temperature on both the as-cast alloys as well as on the heat-treated ones, whereas the DSC measurements are performed during continuous temperature changes. Consequently, some features seen in the measured DSC curves or in the diffraction patterns might not be detected by the other technique as the response to structural phase changes is different.

4.1 Domain I alloys

The diffraction patterns shown in Fig 1 and the reported phases identified in Table 2 show that the two annealing procedures T1 and T3 do not change the overall crystalline structures of the alloys. Only two different structures are observed, namely fcc and hcp. The corresponding diffraction peak position are shown as vertical bars in Figs 1. The only exception is the CCFNPd alloy for which the measured pattern exhibits several extra peaks after the T3 heat treatment implying the presence of a third structure. It was suggested in [10] that these were originating from a slightly distorted fcc structure (actually a monoclinic structure with a very similar lattice constant). This view is supported by DSC results discussed below.

The features observed in the DSC heat flow curves (Fig. 5a and b) at temperatures less than 1200^{o}C for CCFNPd alloy are summarized in Table 3. In order to substantiate the magnitude, the small ones are listed within parenthesis and the trace ones within double parenthesis. The melting temperature is found to be nearly the same in all the heating schemes

and is found in the range 1276±4°C. The identified features are represented by vertical bars in Fig. 5a.

Table 3: Temperatures in °C at which features are identified in the DSC curves recorded for CCFNPd.

Measurement	T_a	T_b	T_c	T_d	T_e	T_f	T_g	T_h
A	580	(717)	793			(1036)		
B	587		((793))		(991)	1057	1110	
C_1	593	(727)	791	916	987	(1041)		
C_2	(561)							
C_3	(590)	(720)	(797)	917	980	(1040)		1190

The as-cast CCFNPd alloy exhibits many structural transformations when heated to 1100^{o}C (scheme C_1). Some of these are reversible and can be seen again during the second heating after heat treatments T1 and T3. The phase transformation occurring at the temperature T_a clearly takes place irrespective of the heat treatments of the alloy. It is very distinct after T1 and T3 but it is rather faint in the C_3 heating. The corresponding phase has obviously grown during the 3h annealing time which shows the influence of both cooling rate annealing time on the alloy phase content. The DSC curves measured in the C sequence are very similar and show that the T1 and the T3 treatments when followed by slow cooling (40K/min) do not affect the alloy phase content significantly. Thus, all structural changes are reversible in this case.

The diffraction measurements indicate that a new phase was created in the CCFNPd alloy after the T3 treatment (Fig 1a). It might be conjectured that this corresponds to the transformation taking place at the temperature T_c. As the transformation probably is of diffusive nature it has been initiated but not completed during the three hours the alloy was kept at 700^{o}C.

It can be concluded that the crystalline structure of alloys classified to belong to domain I does not change during temperature treatments. All identified crystalline phases in this domain are of fcc and/or hcp type (Table 2). Structural changes, both reversible and irreversible, might occur due to different heat treatments but all phases remain of this type. However, the alloy phase content depends on the rate of temperature changes.

4.2 Domain III alloys

Some diffraction patterns measured on alloys that have been classified in [11, 12] to belong to domain III are shown in Fig 2. Only diffraction peak positions corresponding to the two major structures are displayed as vertical bars. Phases present are mainly bcc, $L2_1$ and B2 in as-cast state with appearance of fcc after T1 treatment in some alloy, e.g. CFNAl. It is noticed that the structural content of an alloy is very sensitive to composition. For example, comparing Fig 2a and Fig 2d it is seen that a small change in the Fe and Al content results in a non-existence of the fcc phase in the CFNAl alloy after the T1 treatment. Removing Cr from the CCFNAl alloy (Fig 2c) causes the disappearance of the B2 structure (Fig 2d).

The CFNAl was also investigated by DSC measurements according to the temperature variation schemes mentioned above. The features observed in the DSC heat flow curves shown in Fig 6 are summarized in Table 4. The identified features are represented by vertical bars. The general shapes of the curves are very different from the ones measured for the CCFNAl alloy (see Fig 7) indicating that the temperature behavior is sensitive to the Cr content. A very striking observation is that the melting takes place in two stages after scheme C_3. The sum of areas of the two peaks is close to the areas of the corresponding peaks measured after schemes A and B. This suggests that the alloy consists of two phases after schemes C_1 and C_2. The temperatures at which the melting processes take place T_{m1} and T_{m2} are shown in table 4.

Table 4: Temperature in ^{o}C at which features are identified in the DSC curves recorded for the CFNAl alloy.

Measurement	T_a	T_b	T_c	T_d	T_e	T_f	T_g	T_h	T_{m1}	T_{m2}
A			630	707		(890)		1064		1384
B			644		752			1106		1400
C_1	(405)	(548)	(633)	(684)		(873)	948	(1072)		
C_2		545								
C_3	((475))	(559)			753			(1040)	1274	1389

The DSC curves for as-cast CFNAl alloy (scheme C_1) exhibit more features than for domain I and II alloys but the magnitude of these is considerably smaller. The T1 and T3 heat treatments followed by quench (A and B) seem to stabilize some of the phases. The transformation occurring at the temperature T_c might correspond to the T_b one at about 630^{o}C that was observed for the CCFNAl alloy (see Table 5). Some features disappear when the annealing is followed by a slow cooling (C_3). Thus, the alloy is very sensitive to the rate of cooling.

It can be concluded that the crystalline structure of alloys classified to belong to domain III does not change during temperature treatments. All identified crystalline phases in this domain are of bcc, B2 or $L2_1$ type (Table 2).

The alloy phase content depends on the rate of temperature changes. The T1 and T3 heat treatments followed by quench (A and B) seem to stabilize some of the phases. Some features disappear when the annealing is followed by a slow cooling (C_3). The slow cooling stabilizes only the T_d transformation.

4.3 Domain II alloys

Some diffraction patterns measured for alloys that have been classified in [11, 12] to belong to domain II are shown in Fig 2. All contain structures of both fcc and bcc type irrespective of heat treatments. Only diffraction peak positions corresponding to the two major structures are displayed as vertical bars. Thus, the clearly visible peaks that correspond to the B2 structure in the Figs 2a and 2b are not explicitly shown. There does not seem to be a uniform behavior of the alloys in this domain on any of the heat treatments T1 and T3 in that for some new structures appear and for some not.

From this domain the CCFNAl alloy was selected for DSC measurements according to temperature schemes mentioned above. The measured curves are shown in Fig. 7 and temperatures at which some specific features are observed are summarized in Table 5. The identified features are represented by vertical bars in Fig. 7. The onset of melting was for schemes A and C_3 found to take place at 1350°C while after scheme B it was somewhat higher, at 1363°C.

Table 5: Temperature in °C at which features are identified in the DSC curves recorded for CCFNAl.

Measurement	T_a	T_b	T_c	T_d	T_e	T_f	T_g	T_h
A		627	776		988	1048	1110	
B	((506))	629	757	831	988	((1071))		1165
C_1	(443)	638	754	(850)	(991)	(1056)		
C_2	((527))	630						
C_3		629	(764)	(858)	990	((1056))		

It can be concluded from the shape of the DSC curves that the structure of this alloy is affected more significantly by temperature changes than the CCFNPd belonging to domain I.

Two main transformations occur, one reversible at about 630ºC (T_b in Table 5) and one partly reversible at about 990ºC (T_e in Table 5). The fcc structure observed in the diffraction pattern of this alloy after the T1 annealing and not after the T3 one can thus be correlated to T_e feature in the DSC curve.

It can be concluded that the crystalline structure of alloys classified to belong to domain II change a lot during temperature treatments. This is obvious due to the presence in these alloys of mixed phases, e.g. metastable phases, intermetallics, sigma, etc. These phases naturally grow or transform to more stable phases under heat treatments. Thus, structural changes, both reversible and irreversible, might occur due to different heat treatments.

5. Conclusion

1) All the alloys belonging to a specific domain have been found to have the type of structure in the as-cast state as predicted by the classification in [11, 12]. Thus, in Domain I alloys with fcc or hcp phases are found while the alloys in Domain III contain phases of bcc type. The alloys in Domain II form phases with both fcc and bcc structure as well as other intermetallic phases.

2) Removing Cr from one alloy can drive the alloy from one Domain to another. A small change in the relative Al amount of an alloy can have the same effect. Both these effects are depending on the resulting values of e/a and r [12].

3) The investigated alloys of Domain I exhibit only one type of structure, whatever heat treatment and cooling rate has been used. The microstructure transforms from multi- to almost single-phase under homogenization at T=1100°C. A heat treatment at 700°C leads to additional phases depending on the cooling procedure after annealing.

4) Alloys of Domain II undergo more phase transformations during the different heat treatments than the investigated Domain I alloy. The alloys contain both fcc and bcc phases (being of mixed type) and are still of mixed type after heat treatment. Most of the phases present in as-

cast samples remain after heat treatment at 1100 and 700°C indicating a pronounced structural instability of the alloy with regard to temperature variations. The relative strength of the different phase changes with the rate of cooling.

5) Alloys from Domain III present more transformations in the as cast sample than for domain I and II alloys but these features are much smaller. The 1100 and 700°C heat treatments followed by quench seem to stabilize some of the phases. The alloy phase composition is very sensitive to the rate of cooling.

5) The importance of rate of cooling after annealing at 1100 and 700°C influences the phase composition and their amount. This a very important result for the homogenization procedure often performed on HEAs, depending in the Domain where their compositions are locating them.

6. Acknowledgements

The authors are thankful to Institute Laue-Langevin, Grenoble, France, for awarding beam-time on the D20 diffractometer at the ILL reactor. Thanks are due to N.J.E. Adkins, at The University of Birmingham (UK) for making the CoFeCu alloy investigated in this study. The present work has been carried out within the FP7 European project AccMet NMP4-LA-2011-263206 for. Some of the DSC measurements have been performed on installations founded by the COMET project at Swansea University.

References

[1] J.W. Yeh, S.K. Chen, S.J. Lin, J.Y. Gan, T.S. Chin, T.T. Shun, C.H. Tsau, S.Y. Chang, Nanostructured high-entropy alloys with multiple principal elements: novel alloy design concepts and outcomes, Adv. Eng. Mater. 6 (2004) 299-303. https://doi.org/10.1002/adem.200300567

[2] M.C. Gao, J.W. Yeh, P.K. Liaw, Y. Zhang Y. High-Entropy alloys: Fundamentals and applications, Springer, 2016.

[3] Y. Zhang, T.T Zuo, Z. Tang, M.C Gao, K.A. Dahmen, P.K. Liaw, Z.P. Lu, Microstructures and properties of high-entropy alloys, Prog. Mater. Sci. 61 (2014) 1-93. https://doi.org/10.1016/j.pmatsci.2013.10.001

[4] D.B. Miracle, O.N. Senkov, A critical review of high entropy alloys and related concepts, Acta Mater. 122 (2017) 448–511. https://doi.org/10.1016/j.actamat.2016.08.081

[5] D.B. Miracle, J.D. Miller, O.N. Senkov, C. Woodward, M.D. Uchic, J. Tiley, Exploration and Development of High Entropy Alloys for Structural Applications, Entropy 16 (2014) 494-525. https://doi.org/10.3390/e16010494

[6] O.N. Senkov, J.D. Miller, D.B. Miracle, C. Woodward, Accelerated exploration of multi-principal element alloys with solid solution phases, Nature Comm. 6 (2015) 6529. https://doi.org/10.1038/ncomms7529

[7] X. Yang, Y. Zhang, Prediction of high-entropy stabilized solid-solution in multi-component alloys, Mater. Chem. and Phys., 132 (2012) 233–238. https://doi.org/10.1016/j.matchemphys.2011.11.021

[8] M.H. Tsai, J.W. Yeh, High-entropy alloys: A critical review, Mater. Res. Lett. 2-3 (2014) 107-123. https://doi.org/10.1080/21663831.2014.912690

[9] Z.P Lu, H. Wang, M.W. Chen, I. Baker, J.W. Yeh, C.T. Liu, T.G. Nieh, An assessment on the future development of high-entropy alloys: Summary from a recent workshop, Intermetallics, 66 (2015) 67-76. https://doi.org/10.1016/j.intermet.2015.06.021.

[10] U. Dahlborg, J. Cornide, M. Calvo-Dahlborg, T. Hansen, A. Fitch, Z. Leong, S. Chambreland, R. Goodall. Structure of some CoCrFeNi and CoCrFeNiPdx multicomponent HEA alloys by diffraction techniques. J. Alloys Compds 681 (2016) 330-341. http://dx.doi.org/10.1016/j.jallcom.2016.04.248.

[11] M. Calvo-Dahlborg, S.G.R. Brown. Hume-Rothery for HEA classification and self-organizing map for phases and properties prediction. J. Alloys and Compds 724 (2017) 353-364. http://dx.doi.org/10.1016/j.jallcom.2017.07.074

[12] M. Calvo-Dahlborg, U. Dahlborg, S. G. Brown, J. Juraszek. Influence of the electronic polymorphism of Ni on the classification and design of high entropy alloys. J. Alloys and Compds. Accepted 2020. In press. https://doi.org/10.1016/j.jallcom.2020.153895

[13] C.S. Barrett, T.B. Massalski. Structure of metals, third edition. McGraw-Hill Eds. 1966. P. 306-379.

[14] T.B. Massalski, Comments Concerning Some Features of Phase Diagrams and Phase Transformations, *Materials Transactions* **51** (2010) 583-596. https://doi.org/10.2320/materia.49.192.

[15] E.T. Teatum, K.A. Gschneidner Jr., J.T. Waber, 1968. Report LA-4003. UC-25. Metals, Ceramics and Materials. TID-4500, Los Alamos Scientific Laboratory.

[16] A. Boultif, D. Louër, Powder pattern indexing with the dichotomy method, J. Appl. Cryst. 37 (2004) 724-731.https://doi.org/10.1107/S0021889804014876

[17] M. Calvo-Dahlborg, J. Cornide, U. Dahlborg, S. Chambreland, G.D. Hatton et A. Fones. Structure and microstructural characterization of CoCrFeNiPd High Entropy Alloys. Solid State Phenomena 257 (2016) 72-75. https://www.scientific.net/SSP.257.72

[18] M. Calvo-Dahlborg, J. Cornide, J. Tobola, D. Nguyen-Manh, J. S. Wróbel, J. Juraszek, S. Jouen, U. Dahlborg. Interplay of electronic, structural and magnetic properties as driving feature of high entropy CoCrFeNiPd alloys. J. Phys. D: Applied Phys. 50 (2017) 185002 (12pp). https://doi.org/10.1088/1361-6463/aa62ea